

1     **The genetic architecture of target-site**  
2     **resistance to pyrethroid insecticides in the**  
3     **African malaria vectors *Anopheles***  
4     ***gambiae* and *Anopheles coluzzii***

5     Chris S. Clarkson<sup>1</sup>, Alistair Miles<sup>2,1</sup>, Nicholas J. Harding<sup>2</sup>,  
6     @@TODO<sup>1</sup>, Dominic Kwiatkowski<sup>1,2</sup>, Martin Donnelly<sup>3,1</sup>, and  
7     The *Anopheles gambiae* 1000 Genomes Consortium<sup>4</sup>

8                     <sup>1</sup>Sanger @@TODO

9                     <sup>2</sup>Oxford @@TODO

10                    <sup>3</sup>Liverpool @@TODO

11                    <sup>4</sup>MalariaGEN @@TODO

12                    Work in progress

13                    **Abstract**

14            Resistance to pyrethroid insecticides is a major concern for malaria vector  
15            control, because these are the only compounds approved for use in insecticide-  
16            treated bed-nets (ITNs) and are also widely used for indoor residual spraying  
17            (IRS). Pyrethroids target the voltage-gated sodium channel (VGSC), an es-  
18            sential component of the mosquito nervous system, but mutations in the *Vgsc*

gene can disrupt the activity of these insecticides, inducing a “knock-down resistance” phenotype. Here we use Illumina whole-genome sequence data from phase 1 of the *Anopheles gambiae* 1000 Genomes Project (Ag1000G) to provide a comprehensive account of genetic variation at the *Vgsc* locus in mosquito populations from 8 African countries. In addition to three known resistance variants that alter the protein-coding sequence of the *Vgsc* gene, we describe 19 previously unknown non-synonymous variants at appreciable frequency in one or more populations. For each variant we predict a resistance phenotype based on genetic evidence for recent selection, patterns of linkage between variants, the position of the variant within the protein structure, and experimental evidence from other species. We use analyses of haplotype structure to refine our understanding of the origins and spread of these resistance variants between species and geographical locations. These analyses identify 10 distinct lineages, each of which carries one or more resistance alleles and appears to be undergoing rapid and recent expansion in one or more populations. The most successful and widespread resistance lineage (F1) originates in West Africa and has subsequently spread to countries in Central and Southern Africa. We also reconstruct a putative ancestral haplotype for each lineage, and analyse patterns of recombination to show that lineages are unrelated and thus represent independent outbreaks of resistance. Our data demonstrate that the molecular basis of pyrethroid resistance in African malaria vectors is more complex than previously appreciated, and provide a foundation for the development of new genetic tools to inform insecticide resistance management and track the further spread of resistance.

## Introduction

An estimated 663 million cases of malaria were averted in Africa between 2000 and 2015 due to public health interventions, of which 68% were prevented by insecticide-treated bed-nets (ITNs) and 22% through indoor residual spraying of insecticides (IRS). However, over this same period, insecticide resistance has become increasingly prevalent in malaria vector populations. Four chemical classes of insecticides – organophosphates, carbamates, pyrethroids and organochlorines – are licensed for use

in public health, but only pyrethroids are approved by the World Health Organisation (WHO) for use in ITNs. Pyrethroids are also commonly used for IRS and in agriculture, and mosquito populations are under pressure to evolve molecular mechanisms of pyrethroid resistance. There is evidence that pyrethroid resistance has a direct impact on the effectiveness of ITNs and IRS, although assessing the impact on disease prevalence is difficult and has been hampered by the fact that pyrethroid resistance is now so pervasive that it is nearly impossible to find fully susceptible mosquito populations to serve as controls. Nevertheless, the position of the WHO remains that insecticide resistance poses a grave threat to the future of malaria control in Africa (GPIRM). Improvements are needed in our ability to monitor resistance, and gaps must be filled in our knowledge of the molecular mechanisms of resistance.

The voltage-gated sodium channel (VGSC) is the physiological target of pyrethroids and of the organochlorine DDT. The VGSC protein is integral to the insect nervous system, involved in the transmission of nerve impulses. Both pyrethroids and DDT have a similar mode of action, binding to sites within the protein channel and preventing normal nerve function, causing paralysis (“knock-down”) and then death. However, amino acid substitutions at key positions within the channel can alter the interaction between the channel and the insecticide molecule, and thereby substantially increase the dosage of insecticide required for knock-down. If this tolerance exceeds the dosage present in ITNs or on indoor surfaces following IRS, these interventions may be rendered ineffective. In the African malaria vectors *Anopheles gambiae* and *Anopheles coluzzii*, three substitutions have been found in natural populations and shown to cause pyrethroid and DDT resistance. Two of these substitutions occur in codon 995<sup>1</sup>, with the Leucine → Phenylalanine (L995F) substitution prevalent in West and Central Africa, and the Leucine → Serine (L995S) substitution found in Central and East Africa. A third variant N1570Y has been

---

<sup>1</sup>Codon numbering is given here relative to transcript @@TODO as defined in the AgamP4.@@N gene annotations. A mapping of codon numbers from @@TRANSCRIPT to *Musca domestica* @@TRANSCRIPT is given in Table 1.

77 found in association with L995F in Central Africa and shown to increase resistance  
78 above L995F alone.

79 Target-site resistance to pyrethroids and DDT has also been studied in a range  
80 of other insect species, including disease vectors as well as domestic and crop pests.  
81 Because of its essential function, the VGSC protein is highly conserved across in-  
82 sect species, and knowledge gained from one species is relevant to another. Many  
83 resistance-associated variants have been described in these other species, and thus  
84 there are many possible amino acid substitutions that could induce a resistance  
85 phenotype in malaria vectors, other than the known variants in codons 995 and  
86 1570. Some of these variants are within the trans-membrane channel, and thus may  
87 directly interact with insecticide molecules. However, functional studies have also  
88 demonstrated that variants within internal linker domains can substantially enhance  
89 the the level of resistance, when present in combination with channel modifications.  
90 Most previous studies of *An. gambiae* and/or *An. coluzzii* have performed targeted  
91 sequencing of small regions within the gene, and there has been no comprehensive  
92 survey of variation across the entire gene in multiple populations.

93 Insecticide resistance monitoring in malaria vector populations now often incor-  
94 porates some form of genetic assay to detect the allele present at *Vgsc* codon 995.  
95 Both alleles are present at high frequency in multiple geographical locations, and the  
96 L995F allele is present in both *An. gambiae* and *An. coluzzii*. The extent of mos-  
97 quito migration remains an open question, however mosquitoes do travel between  
98 different locations and have the potential to spread resistance alleles from one pop-  
99 ulation to another (adaptive gene flow). Hybridization between mosquito species  
100 also occurs and has the potential to transfer resistance alleles between species (ad-  
101 aptive introgression). Studies in West African have shown that the L995F allele  
102 has been transferred from *An. gambiae* into *An. coluzzii* populations. A resist-  
103 ance allele may also arise independently in multiple populations, either because of  
104 multiple mutational events occurring after insecticides are introduced (selection on  
105 new mutations), or because resistance alleles were already present at low frequency

106 in mosquito populations prior to insecticide use (selection on standing variation).  
107 Previous studies have found evidence that the L995F allele occurs on several differ-  
108 ent genetic backgrounds, suggesting multiple origins of resistance. However, these  
109 studies have used information from only a small region of the gene, and have limited  
110 resolution to make inferences about geographical origins or history of spread. Bet-  
111 ter information about the origins and spread of resistance could improve insecticide  
112 resistance monitoring and inform strategies for insecticide resistance management.

113 Here we provide a detailed and comprehensive account of genetic variation within  
114 the *Vgsc* gene using data from phase 1 of the *Anopheles gambiae* 1000 Genomes  
115 Project (Ag1000G). We use genotype and haplotype data derived from whole-genome  
116 Illumina sequencing of 765 individual mosquitoes collected from natural populations  
117 in 8 African countries to survey genetic diversity and study the evolutionary and  
118 demographic history of insecticide resistance at the *Vgsc* locus. Our results reveal  
119 an unexpected diversity of molecular mechanisms of resistance, and shed new light  
120 on the evolutionary processes underlying the rapid increase in the prevalence of  
121 resistance across multiple mosquito populations.

## 122 Results

### 123 Identification of resistance alleles

124 To identify single nucleotide polymorphisms (SNPs) with a potentially functional  
125 role in pyrethroid resistance, we extracted SNPs from the Ag1000G phase 1 data  
126 resource that alter the amino acid sequence of the VGSC protein, and computed  
127 their allele frequencies among 9 populations defined by species and country of origin.  
128 SNPs that confer resistance are expected to increase in frequency under selective  
129 pressure, and we refined the list of potentially functional SNPs to retain only those at  
130 an appreciable frequency (>5%) in one or more populations (Table 1). The resulting  
131 list comprises 20 SNPs, including the known L995F, L995S and N1570Y variants, and  
132 a further 17 SNPs not previously described in these species. We reported 15 of these

133 novel SNPs in our initial analysis of the Ag1000G phase 1 data (@@REF Ag1000G),  
 134 and we extend the analyses here to incorporate two tri-allelic SNPs affecting codons  
 135 402 and 410.

136 The two alleles in codon 995 are clearly the main drivers of resistance at this locus,  
 137 with the L995F allele at high frequency in populations of both species from West,  
 138 Central and Southern Africa, and the L995S allele at high frequency among *An. gam-*  
 139 *biae* populations from Central and East Africa (Table 1; @@REF Ag1000G). Both  
 140 alleles were present in populations sampled from Cameroon and Gabon, including  
 141 some individuals with a hybrid L995F/S genotype. Within these populations, the  
 142 L995F and L995S alleles were (@@TODO were not?) in Hardy-Weinberg equilibrium  
 143 ( $P=@@$ ), thus there does not (@@does?) appear to be selection against hybrids.

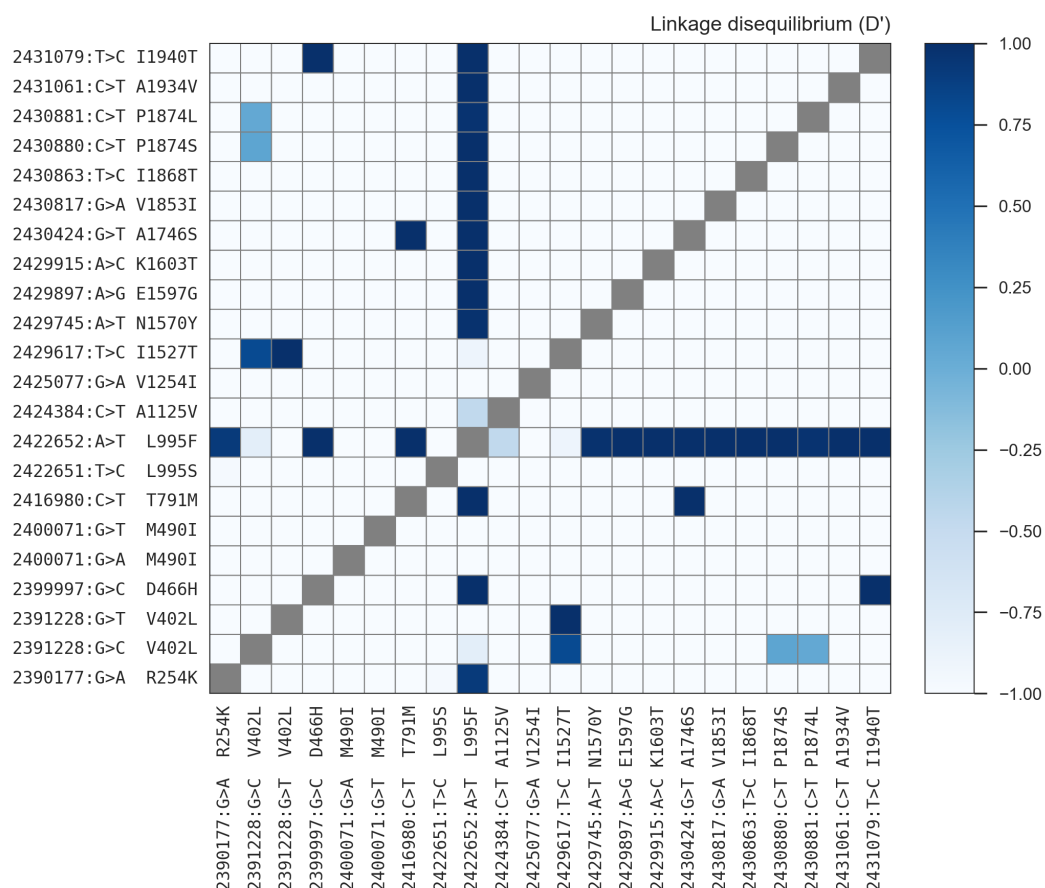


**Figure 1. Linkage disequilibrium between non-synonymous variants.** A value of 1 indicates that the two variants always occur in combination, and conversely a value of -1 indicates that the two variants never occur in combination. @TODO nuance this?

Variant			Population allele frequency (%)										Function	
Position <sup>1</sup>	<i>Ag</i> <sup>2</sup>	<i>Ma</i> <sup>3</sup>	AO <i>Ac</i>	BF <i>Ac</i>	GN <i>Ag</i>	BF <i>Ag</i>	CM <i>Ag</i>	GA <i>Ag</i>	UG <i>Ag</i>	KE	GW	Domain <sup>4</sup>	Resistance phenotype <sup>5</sup>	
2,390,177 G>A	R254K	R261	0	0	0	0	32	21	0	0	0	IN (I.S4-I.S5)	L995F enhancer (predicted)	
2,391,228 G>C	V402L	V410	0	7	0	0	0	0	0	0	0	TM (I.S6)	I1527T enhancer (predicted)	
2,391,228 G>T	V402L	V410	0	7	0	0	0	0	0	0	0	TM (I.S6)	I1527T enhancer (predicted)	
2,399,997 G>C	D466H	-	0	0	0	0	7	0	0	0	0	IN (I.S6-II.S1)	L995F enhancer (predicted)	
2,400,071 G>A	M490I	M508	0	0	0	0	0	0	0	18	0	IN (I.S6-II.S1)	none (predicted)	
2,400,071 G>T	M490I	M508	0	0	0	0	0	0	0	0	0	IN (I.S6-II.S1)	none (predicted)	
2,416,980 C>T	T791M	T810	0	1	13	14	0	0	0	0	0	TM (II.S1)	L995F enhancer (predicted)	
2,422,651 T>C	L995S	L1014	0	0	0	0	15	64	100	76	0	TM (II.S6)	driver	
2,422,652 A>T	L995F	L1014	86	85	100	100	53	36	0	0	0	TM (II.S6)	driver	
2,424,384 C>T	A1125V	K1133	9	0	0	0	0	0	0	0	0	IN (II.S6-III.S1)	none (predicted)	
2,425,077 G>A	V1254I	I1262	0	0	0	0	0	0	0	0	5	IN (II.S6-III.S1)	none (predicted)	
2,429,617 T>C	I1527T	I1532	0	14	0	0	0	0	0	0	0	TM (III.S6)	driver (predicted)	
2,429,745 A>T*	N1570Y	N1575	0	26	10	22	6	0	0	0	0	IN (III.S6-IV.S1)	L995F enhancer	
2,429,897 A>G	E1597G	E1602	0	0	6	4	0	0	0	0	0	IN (III.S6-IV.S1)	L995F enhancer (predicted)	
2,429,915 A>C	K1603T	K1608	0	5	0	0	0	0	0	0	0	TM (IV.S1)	L995F enhancer (predicted)	
2,430,424 G>T	A1746S	A1751	0	0	11	13	0	0	0	0	0	TM (IV.S5)	L995F enhancer (predicted)	
2,430,817 G>A	V1853I	V1858	0	0	8	5	0	0	0	0	0	IN (IV.S6-)	L995F enhancer (predicted)	
2,430,863 T>C	I1868T	I1873	0	0	18	25	0	0	0	0	0	IN (IV.S6-)	L995F enhancer (predicted)	
2,430,880 C>T	P1874S	P1879	0	21	0	0	0	0	0	0	0	IN (IV.S6-)	L995F enhancer (predicted)	
2,430,881 C>T	P1874L	P1879	0	7	45	26	0	0	0	0	0	IN (IV.S6-)	L995F enhancer (predicted)	
2,431,061 C>T	A1934V	A1939	0	12	0	0	0	0	0	0	0	IN (IV.S6-)	L995F enhancer (predicted)	
2,431,079 T>C	I1940T	I1945	0	4	0	0	7	0	0	0	0	IN (IV.S6-)	L995F enhancer (predicted)	

<sup>1</sup> Position relative to the AgamP3 reference sequence, chromosome arm 2L. Variants marked with an asterisk (\*) failed conservative variant filters applied genome-wide in the Ag1000G phase 1 AR3 callset, but appeared sound on manual inspection of read alignments.

<sup>2</sup> Codon numbering according to *Anopheles gambiae* transcript AGAP004707-RA in geneset AgamP4.4.

<sup>3</sup> Codon numbering according to *Musca domestica* EMBL accession X96668 [1].

<sup>4</sup> Position of the variant within the protein. IN=internal domain; TM=trans-membrane domain. The protein contains four homologous repeats (I-IV), each having six transmembrane segments (1-6). Codes in parentheses identify the specific domain, e.g., “I.S4” refers to trans-membrane segment 4 in repeat I, and “IS4-IS5” refers to the linker segment between I.S4 and I.S5.

<sup>5</sup> Phenotype predictions are based on population genetic evidence and have not been confirmed experimentally.

**Table 1. Non-synonymous nucleotide variation in the voltage-gated sodium channel gene.** AO=Angola; BF=Burkina Faso; GN=Guinea; CM=Cameroon; GA=Gabon; UG=Uganda; KE=Kenya; GW=Guinea-Bissau; *Ac*=*An. coluzzii*; *Ag*=*An. gambiae*. All variants are at 5% frequency or above in one or more of the 9 Ag1000G phase 1 populations, with the exception of 2,400,071 G>T which is only found in the CM*Ag* population at 0.4% frequency but is included because another mutation (2,400,071 G>A) is found at the same position causing the same amino acid substitution (M490I).

144 The I1527T allele is present in *An. coluzzii* from Burkina Faso at 14% frequency,  
 145 and there is evidence that haplotypes carrying this allele have been positively selec-  
 146 ted (@@REF Ag1000G). Codon 1527 occurs within trans-membrane domain segment  
 147 III.S6, immediately adjacent to a second predicted binding pocket for pyrethroid  
 148 molecules, thus it is plausible that I1527T could alter insecticide binding (@@REF  
 149 Dong). We also found that the two variant alleles affecting codon 402, both of  
 150 which induce a V402L substitution, were in strong linkage with I1527T ( $D' > @@N$ ;  
 151 Figure @@LD), and almost all haplotypes carrying I1527T also carried a V402L  
 152 substitution. The most parsimonious explanation for this pattern of linkage is that  
 153 the I1527T mutation occurred first, and mutations in codon 402 subsequently arose  
 154 on this genetic background. Codon 402 also occurs within a trans-membrane seg-  
 155 ment (I.S6), and the V402L substitution has by itself been shown experimentally to  
 156 increase pyrethroid resistance in @@species and *Xenopus* oocytes (@@REFs). How-  
 157 ever, because V402L appears secondary to I1527T in our cohort, we classify I1527T  
 158 as a putative resistance driver and V402L as a putative enhancer. Because of the lim-  
 159 ited geographical distribution of these alleles, we hypothesize that the I1527T+V402L  
 160 combination represents a pyrethroid resistance allele that arose in West African *An.*  
 161 *coluzzii* populations; however, the L995F allele is at higher frequency (85%) in our  
 162 Burkina Faso *An. coluzzii* population, and is known to be increasing in frequency  
 163 (@@REFs), therefore L995F may provide a stronger resistance phenotype and is  
 164 replacing I1527T+V402L in these populations.

165 Of the other 16 SNPs, 13 occurred almost exclusively in combination with L995F  
 166 (Figure @@; @@REF Ag1000G). These include the N1570Y allele, known to enhance  
 167 pyrethroid resistance in *An. gambiae* in combination with L995F. These also include  
 168 two variants in codon 1874 (P1874S, P1874L). P1874S has previously been found in a  
 169 colony of the crop pest *Plutoblah blahdiblah* with a pyrethroid resistance phenotype,  
 170 but has not been shown to confer resistance experimentally. 10 of these variants,  
 171 including N1570Y and P1874S/L, occur within internal linker domains of the pro-  
 172 tein, and so fit the model of variants that may enhance or compensate for the driver



173 phenotype by modifying channel gating behaviour (@@CHECK; @@REFs). The  
174 remaining 3 variants are within trans-membrane domains, and so may enhance res-  
175 istance by @@TODO how. Because of the tight linkage between these 13 SNPs and  
176 the L995F allele, we classify all as putative L995F enhancers, although experimental  
177 work is required to confirm a resistance phenotype.

178 The remaining 3 variants (M490I, A1125V, V1254I) do not occur in combination  
179 with any known resistance allele, and do not appear to be associated with haplotypes  
180 under selection (@@REF Ag1000G). A possible exception is the M490I allele found  
181 at 18% frequency in the Kenyan population, although the fact that this population  
182 has experienced a recent population crash makes it difficult to test for evidence of  
183 selection at this locus. All 3 variants occur in internal linker domains, and so do not  
184 fit the model of a resistance driver, although experimental work is required to rule  
185 out a resistance phenotype.

## 186 **Origins and spread of resistance alleles**

187 Although it is well-known that pyrethroid resistance is becoming increasingly pre-  
188 valent in malaria vector populations across Africa, it has not previously been clear  
189 whether this increase in prevalence is being driven primarily by the spread of resist-  
190 ance alleles from one location to another via mosquito migration, or by resistance  
191 alleles emerging independently and simultaneously in multiple locations, or by a com-  
192 bination of both processes. In our initial analyses of haplotype data from Ag1000G  
193 phase 1 (@@REF Ag1000G), we used a clustering approach based on genetic dis-  
194 tance to identify 10 haplotype clusters at the *Vgsc* locus carrying a known resistance  
195 driver allele, of which five clusters carried L995F (labelled F1-F5) and a further five  
196 clusters carried L995S (labelled S1-S5). Within each cluster, haplotypes were nearly  
197 identical across the entire @@70 kbp span of the *Vgsc* gene, and therefore represent a  
198 collection of haplotypes with a very recent common ancestor. Within some of these  
199 clusters, we found haplotypes from mosquitoes collected from different geograph-  
200 ical locations, demonstrating that adaptive gene flow has occurred between these

201 locations. Specifically, cluster F1 contained haplotypes from Guinea, Burkina Faso,  
 202 Cameroon and Angola; clusters @@ each contained haplotypes from both Cameroon  
 203 and Gabon; and cluster @@ contained haplotypes from both Uganda and Kenya.  
 204 The F1 cluster also contained haplotypes from both *An. gambiae* and *An. coluzzii*,  
 205 demonstrating that adaptive introgression had occurred. We also used analyses of  
 206 haplotype clustering on the flanks of the *Vgsc* gene to provide evidence that each of  
 207 these haplotype clusters represents an independent outbreak of resistance, with the  
 208 exception of clusters S4 and S5 which appear to be recently derived from the same  
 209 ancestor. In this section we present several new analyses to confirm and extend our  
 210 initial findings regarding the origins and spread of *Vgsc* resistance alleles.

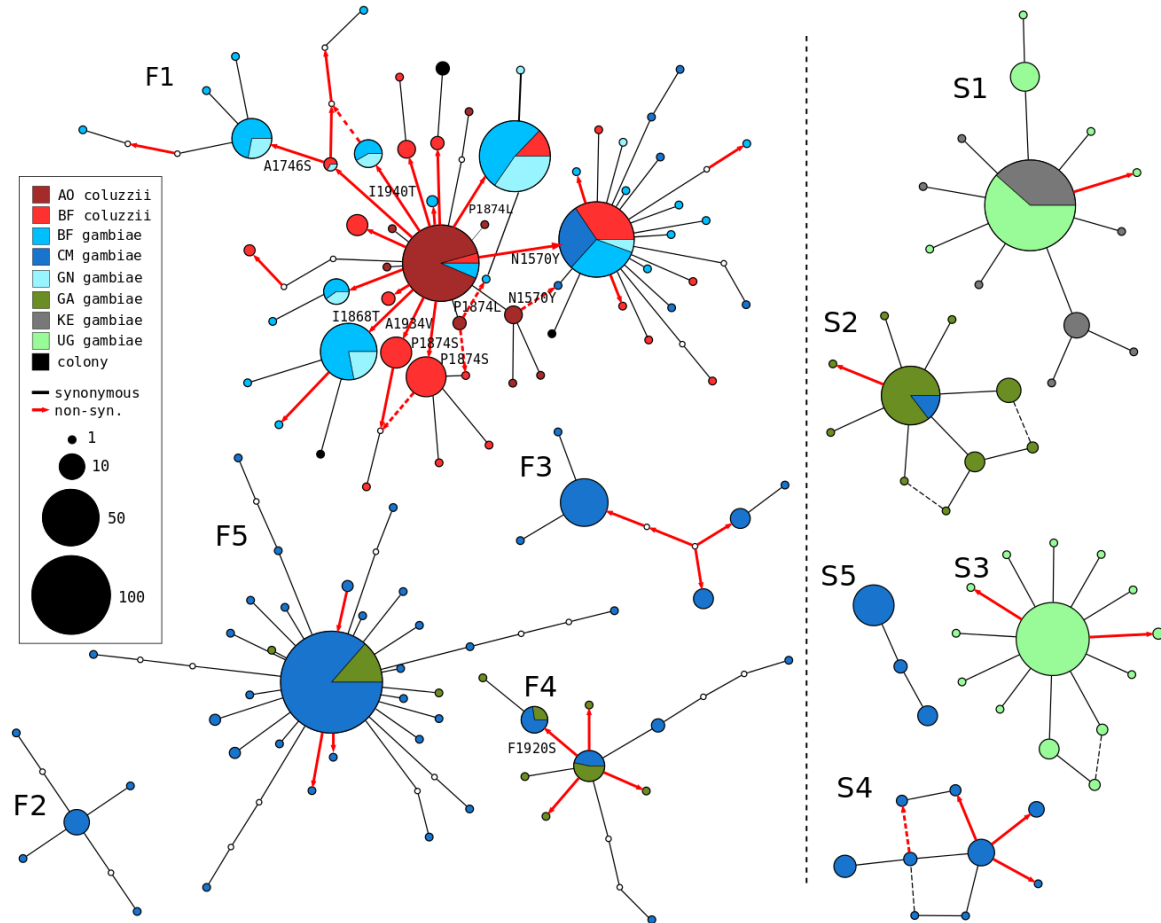


**Figure 2. Haplotype networks.** @@TODO redo the figure. @@TODO annotate non-syn edges in cluster F3. @@TODO mention if any clusters fixed for non-syn variants so not shown. @@TODO annotate other non-syn edges, e.g., in S4?

211 To provide an alternative view of the genetic similarity between haplotypes car-  
 212 rying known or predicted resistance driver alleles, we used haplotype data across all  
 213 1710 (@@CHECK) SNPs within the *Vgsc* open reading frame to construct median-  
 214 joining networks (Figure 2). We constructed these networks up to a maximum  
 215 distance of @@4 SNP differences, to ensure that each connected component in the  
 216 resulting networks represents a collection of haplotypes with a recent common an-  
 217 cestor, and thus which is also likely to be minimally affected by recombination within  
 218 the gene. For L995F, the resulting network confirms the presence of five distinct  
 219 clusters of closely-related haplotypes, with close correspondance to the clusters F1-  
 220 F5 identified previously (@@REF Ag1000G). The haplotype network for cluster F1  
 221 brings into sharp relief the explosive evolution of secondary amino acid substitutions  
 222 within the F1 lineage, providing further evidence that they play a functional role in  
 223 enhancing the L995F resistance phenotype. The distribution of secondary variants  
 224 within the F1 network also allows us to infer multiple introgression events between  
 225 the two species. @@TODO details of which variants are found in both species.

226 The L995S network also confirms five distinct clusters, in concordance with our  
 227 previous analysis. The contrast between the haplotype networks for the L995F and  
 228 L995S alleles is striking, because of the near-total absence of any non-synonymous  
 229 variants within the L995S networks. As we reported previously, there is a highly sig-  
 230 nificant enrichment for non-synonymous variation among haplotypes carrying L995F  
 231 relative to haplotypes with L995S. This difference is the basis for our prediction that  
 232 all of the secondary non-synonymous variants found at appreciable frequency among  
 233 L995F haplotypes are likely to enhance the resistance phenotype, rather than being  
 234 deleterious or neutral variants that are hitch-hiking on selective sweeps for the driver  
 235 allele, because hitch-hiking should be similar for both L995F and L995S.

236 A limitation of both the hierarchical clustering and network analyses is that they  
 237 only leverage information from within the *Vgsc* gene. Because they are relying on  
 238 estimates of genetic distance from within a relatively small genome region, they have  
 239 limited resolution to infer very recent events, because insufficient time has elapsed

for mutations to occur. This means that, within each of the lineages we have identified where adaptive gene flow has occurred, the analyses provide little information about the direction or relative timing of gene flow events. To improve our resolution to infer recent events, we used information about the extent of haplotype sharing on both flanks of the gene. For each pair of haplotypes, we used a heuristic approach to estimate the length of the region shared identical by descent (IBD) between two haplotypes, extending both upstream and downstream of the gene, and to estimate the number of mutations that have accumulated within IBD regions since the most recent common ancestor (MRCA). We then combined the information about IBD length and number of mutations to estimate the time to MRCA or "age" for each pair of haplotypes. We used hierarchical clustering to visualise the overall age structure (Figure 3), and also analysed the distribution of ages within and between different collections of haplotypes (Figure @@REF). We caution that these analyses are relatively crude, and could be improved in a number of ways. However, estimating haplotype age and local genealogy is a very active research area, and we use a heuristic approach here to provide an initial view into the data. We also caution that although the estimated ages are in units of generations, these estimates have

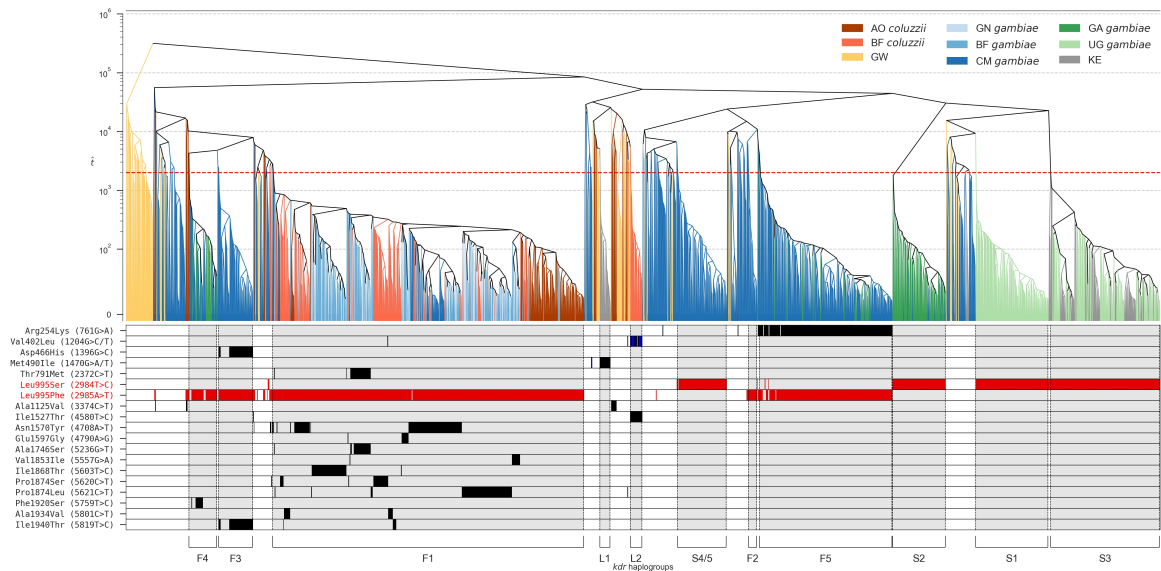


**Figure 3. Clustering of haplotypes by age.** @@TODO bigger font. @@TODO change "kdr haplogroups" to something else. @@TODO yticks to show number of haplotypes.

not been calibrated, and so cannot be taken as accurate absolute values. They can, however, be compared with each other, to explore the relative age of different events.

A key feature of the overall distribution of haplotype ages is that it is bimodal, with a minor mode of haplotypes coalescing recently, and a major mode coalescing further in the past (Figure @@REF). This is expected at a locus experiencing recent positive selection and multiple selective sweeps. Within each sweep, all haplotypes share a very recent common ancestor, but between sweeps and among haplotypes without any resistance allele, genealogies reflect a more even distribution of ancestry. This overall bimodal distribution is also not simply a reflection of geographical population structure, because the same bimodality is observed within several populations (Figure @@REF). We take the midpoint between these two modes as an estimate for the maximum age of selective sweeps at this locus. When we then cut the haplotype tree at this age, and take the 11 largest clades, we find that the resulting clades are highly concordant with the clustering and network analyses based on genetic distance within the gene (Figure 3). Clusters F1-F5 are recapitulated, as are clusters S1-S4, with S4 and S5 merged into a single cluster reflecting their shared ancestry as discovered from previous analyses. We also label a new cluster "L@@" representing the lineage of haplotypes carrying the I1527T allele in combination with one or the other V402L allele. @@TODO what to say about the other "L@@" cluster?

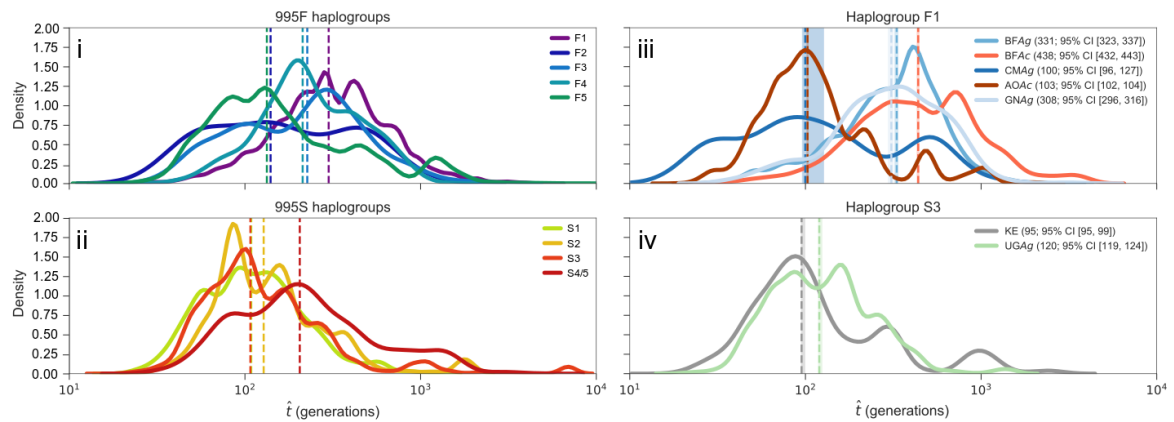


**Figure 4. Haplotype age distributions.** @@TODO rethink what goes in here, also if this needs to be here or can go to supplementary.

277 Using these estimates for haplotype age, we draw some tentative conclusions re-  
278 garding the history of these resistance outbreaks. @@TODO describe evidence for  
279 direction of spread within spreading haplogroups.

280 @@TODO talk about reconstructing ancestral haplotypes and studying recom-  
281 bination. Does this need a new sub-section? If so, what's the title?

282 @@TODO other part of recombination figure – both go to supplementary?

## 283 Discussion

284 @@TODO

## 285 Methods

286 @@TODO

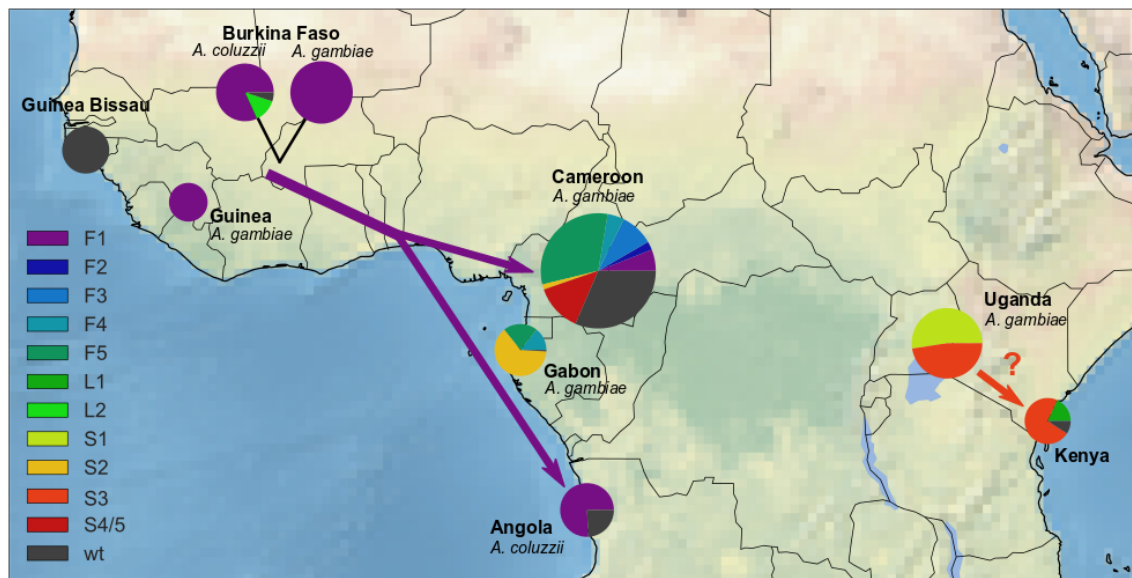
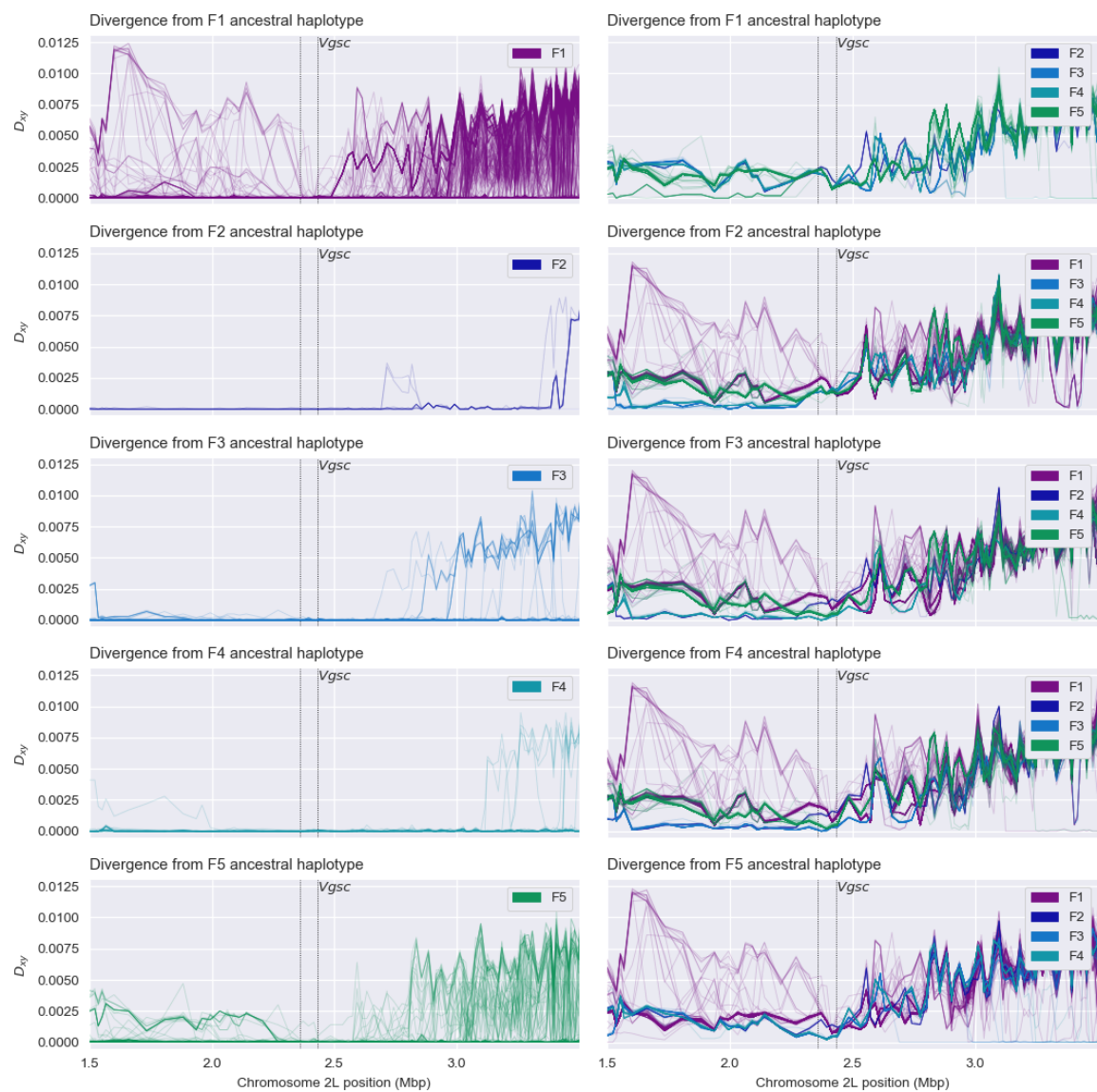


Figure 5. Geographical distribution of resistance haplogroups.

287 **References**

288 [1] Martin S Williamson et al. ‘Identification of mutations in the houseflypara-type  
 289 sodium channel gene associated with knockdown resistance (kdr) to pyrethroid  
 290 insecticides’. In: *Molecular and General Genetics MGG* 252.1 (1996), pp. 51–60.



**Figure 6. Recombination.** @@TODO legend